Materials With Required Dielectric Properties: Computational Development and Production of Polymer-Ceramic Composites

Sébastien Vaucher,[1] Vadim V. Yakovlev ![ORCID],[2] Hannah Yeung[3]

[1]Laboratory for Advanced Materials Processing, EMPA – Swiss Federal Laboratories for Materials Science and Technology, Thun, Switzerland

[2]Department of Mathematical Sciences, Worcester Polytechnic Institute, Worcester, Massachusetts

[3]Department of Mechanical Engineering, Worcester Polytechnic Institute, Worcester, Massachusetts

Many applications in wireless communication, microelectronics, and microwave power engineering rely on dielectrics with particular dielectric properties. This article proposes an original approach that can be used for producing materials with required complex permittivity. The technique is based on an inverted power-law mixing rule model computing volume fractions in which three or more prime materials should be taken to get in the resulting homogeneous mixture the required dielectric properties. Functionality of the approach is demonstrated by production of composites from a polymer matrix (polymethyl methacrylate) and two inorganic fillers (silicon and alumina). The composites are made by mechanically mixing the powders and axially hot-pressing and cooling the mixture. Complex permittivity of the samples is measured by a split-post resonator method. Experimental data on dielectric properties of the samples help calibrate the technique; for the used powders, the Looyenga power-law model is found to be most adequate. In the produced samples, the target values of dielectric constant are reached with a higher precision than the ones of the loss factor; however, analysis of the production process and error propagation in the computations suggest that deviations of the resultant complex permittivity fall in the anticipated ranges. Features and issues of both computational and production parts of the technique are finally discussed. POLYM. ENG. SCI., 58:319–326, 2018. © 2017 Society of Plastics Engineers

INTRODUCTION

Numerous scientific and industrial applications in wireless communications, telemetry, biomedical engineering, material processing and process control include propagation/interaction of electromagnetic fields through/with the media. Dielectric properties of those media are critically important for efficient operations of corresponding systems and apparatuses [1,2].

Microwave power engineering is a field in which dielectric materials and their properties play a particularly crucial role. With the development and innovations in the related technologies currently on the rise (see, e.g., [3–8]), the designers of systems for different applications continue to struggle with an intrinsic non-uniformity of microwave heating [9–12]. Among many methods aiming to homogenize the process, there is a group of techniques attempting to improve the heating profile through a deformation of the pattern of the electric field by partially filling the cavity with appropriate dielectric slabs (e.g., [13,14]). Recently, this approach has been revisited, and an original optimization-based technique [15,16] was proposed for determination of geometry and dielectric properties of a dielectric insert which, when placed inside a microwave applicator, maximizes the level of uniformity in the distribution of dissipated power within the processed material. Although proposed for application in a specific technology exploiting very fast heating (and thus concerned with patterns of dissipated power rather than temperature), this technique has a clear potential for using in an array of applications in microwave-assisted chemistry, high temperature microwave processing of materials, microwave treatment of food, and other applications, especially those employing controllable solid-state generators [8,17]. Beyond microwave power technologies, materials with particular (high or low) dielectric properties are required in many applications in wireless communication, microelectronics, and microwave processing [1,18–20].

The key element of the technique [15,16] is a supplementary dielectric insert characterized by geometrical parameters and complex permittivity determined from the preceding optimization. However, while machining any shape of the insert may be not a problem (particularly, given contemporary additive manufacturing technologies), the material with required dielectric constant ε' and the loss factor ε'' may not be readily available. This may make practical utilization of this otherwise promising technique problematic.

In this article, we introduce an approach which can be used for producing materials characterized by a desired complex permittivity. The approach relies on the inverted power-law mixing rule for three or more prime materials with different (known) complex permittivity. A composite is produced as a homogeneous mixture of those prime materials which are taken in volume fractions determined from that model, and the resulting complex permittivity is verified by measurement. The production method is presumed to be appropriate for participating components: for low dielectric constants, various polymer substances appear to be suitable, whereas for higher dielectric constants, ceramic materials are likely to be used. At the initial stage of the development of the proposed approach that is reported in this article we deal with a polymer matrix loaded with two inorganic fillers and, as such, are limited to relatively low values of dielectric constant of the target mixture.

We introduce the inverted mixing rules for several power-law models known from literature and experimentally demonstrate functionality of the proposed approach. The samples are made by mechanically mixing silicon, alumina, and polymethyl methacrylate (PMMA) powders and axially hot-pressing and

cooling the mixture. The inverted mixing rule based on the Looyenga (a.k.a. Landau-Lifshitz) model is found to be most adequate for the composites made of powder prime materials and is used for determination of volume fractions. Complex permittivity of the produced composites is measured by a split-post resonator method. This method is also used for determining complex permittivity of the prime materials by measuring the hot-pressed samples made of pure PMMA and of binary mixtures of PMMA with silicon and alumina (followed by computation of ε' and ε'' of the latter using the inverted Looyenga model). Features and issues of both computational and production parts of the technique are discussed. In the produced samples, the target values of dielectric constant are reached with a higher precision that the ones of the loss factor. We explain this divergence by physical properties of silicon powder (including its low volume fractions in the mixtures) and suggest that it can be overcome in alternative implementations of the technique. Uncertainties in computation of dielectric properties of the experimental samples by the Looyenga model due to error propagation are also calculated, and it is concluded that, ultimately, deviations of the resulting ε''_m fall in the anticipated ranges.

COMPUTATIONAL TECHNIQUE

With multiple mixing rules used in modeling of heterogeneous materials [21–24], in our approach, determination of volume fractions of the prime materials relies on the power-law mixing rule [21,23] which can be written for complex permittivity of the mixture $\varepsilon_m = \varepsilon_m' - j\varepsilon_m''$ as

$$\varepsilon_m^{\alpha} = \sum_{i=1}^{n} V_1 \varepsilon_i^{\alpha}, \ \sum_{i=1}^{n} V_i = 1, \ n \geq 3 \qquad (1)$$

where n is the number of prime materials with complex permittivities ε_i, and V_i are their volume fractions. The rule (1) takes shapes of different models for the values of α in the interval between the Wiener boundary values [−1, 1] [23,25], namely, −1 (series model) [23], 0 (logarithmic/Lichtenecker model) [21,26], 1/2 (refractive/Birchak/Kraszewski model) [21,27,28], 1/3 (Looyenga/Landau-Lifshitz model) [21,29,30], $(V_1 - 0.35)$ (Wakino model) [23,31], $(1.65V_1 + 0.265,$ for $V_1 \leq 0.25)$ (Stölzle model) [32], and 1 (parallel model) [23,25]. With different α the rule (1) is applicable to a wide array of media characterized by different structure/topology (including isotropy and anisotropy) and different shapes/orientations of the constitutive particles in the mixture [21,23].

Interpreting ε_m to be the required complex permittivity and considering three prime materials with known ε_1, ε_2, and ε_3 (i.e., $n = 3$, $V_3 = 1 - V_1 - V_2$), Eq. 1 can be re-written as

$$AV = B \qquad (2)$$

where

$$A = \begin{bmatrix} \varepsilon_1'^{\alpha} - \varepsilon_3'^{\alpha} & \varepsilon_2'^{\alpha} - \varepsilon_3'^{\alpha} \\ \varepsilon_1''^{\alpha} - \varepsilon_3''^{\alpha} & \varepsilon_2''^{\alpha} - \varepsilon_3''^{\alpha} \end{bmatrix}, \ V = \begin{bmatrix} V_1 \\ V_2 \end{bmatrix}, \ B = \begin{bmatrix} \varepsilon_m'^{\alpha} - \varepsilon_3'^{\alpha} \\ \varepsilon_m''^{\alpha} - \varepsilon_3''^{\alpha} \end{bmatrix} \qquad (3)$$

Solving (2) by Gaussian elimination, one determines the volume fractions in which the three prime materials should be taken to lead to a homogeneous mixture with the required ε_m.
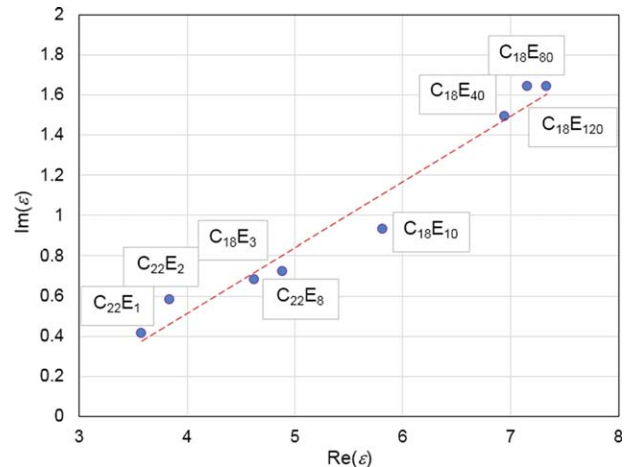

FIG. 1. Values of complex permittivity of the monoalkyl ethers in Table 1 [33]. [Color figure can be viewed at wileyonlinelibrary.com]

To ensure that the solution of (2) makes physical sense (i.e., $0 \leq V_{1,2} \leq 1$) and the target mixture is achievable, the prime materials should be appropriately chosen. Their complex permittivity should correspond to the vertices forming a curvilinear domain on the complex permittivity plane ($\mathrm{Re}(\varepsilon)$, $\mathrm{Im}(\varepsilon)$) that encloses the target value ε_m. The boundaries of the allowable domain are described by three curves with the coordinates:

$$\left(\varepsilon'_{m12}, \ \varepsilon''_{m12} \right) = \left([V_1 \varepsilon_1'^{\alpha} + V_2 \varepsilon_2'^{\alpha}]^{\frac{1}{\alpha}}, \ [V_1 \varepsilon_1''^{\alpha} + V_2 \varepsilon_2''^{\alpha}]^{\frac{1}{\alpha}} \right) \qquad (4a)$$

$$\left(\varepsilon'_{m23}, \ \varepsilon''_{m23} \right) = \left([V_2 \varepsilon_2'^{\alpha} + V_3 \varepsilon_3'^{\alpha}]^{\frac{1}{\alpha}}, \ [V_2 \varepsilon_2''^{\alpha} + V_3 \varepsilon_3''^{\alpha}]^{\frac{1}{\alpha}} \right) \qquad (4b)$$

$$\left(\varepsilon'_{m31}, \ \varepsilon''_{m31} \right) = \left([V_3 \varepsilon_3'^{\alpha} + V_1 \varepsilon_1'^{\alpha}]^{\frac{1}{\alpha}}, \ [V_3 \varepsilon_3''^{\alpha} + V_1 \varepsilon_1''^{\alpha}]^{\frac{1}{\alpha}} \right) \qquad (4c)$$

where ε_{m12}, ε_{m23}, ε_{m31} are complex permittivities of the binary mixtures of materials $1 + 2$, $2 + 3$, and $3 + 1$, respectively.

The described computational technique is exemplified by the following. Figure 1 and Table 1 introduce a set of monoalkyl ethers of polyethylene glycol [33] that is characterized by complex permittivity controlled by the ratio of microwave transparent to microwave absorbing molecular fragments. It is seen that these substances form on the complex permittivity plane a cluster of points closely aligned with a straight line. This means that a mixture of any materials from Table 1 may be characterized by points also very near that line. Diverging from it may be possible by mixing two materials from that set with a component of different molecular structure (and thus notably different

TABLE 1. Monoalkyl ethers of polyethylene glycol (C_nE_m) [33].

Chemical structure	Symbolic expression
$H(CH_2)_{22}\text{-}(OCH_2CH_2)OH$	$C_{22}E_1$
$H(CH_2)_{22}\text{-}(OCH_2CH_2)_2OH$	$C_{22}E_2$
$H(CH_2)_{18}\text{-}(OCH_2CH_2)_3OH$	$C_{18}E_3$
$H(CH_2)_{22}\text{-}(OCH_2CH_2)_8OH$	$C_{22}E_8$
$H(CH_2)_{18}\text{-}(OCH_2CH_2)_{10}OH$	$C_{18}E_{10}$
$H(CH_2)_{18}\text{-}(OCH_2CH_2)_{40}OH$	$C_{18}E_{40}$
$H(CH_2)_{18}\text{-}(OCH_2CH_2)_{80}OH$	$C_{18}E_{80}$
$H(CH_2)_{18}\text{-}(OCH_2CH_2)_{120}OH$	$C_{18}E_{120}$

TABLE 2. Conventional third prime materials to supplement two mono-alkyl ethers of polyethylene glycol (Table 1) in the illustrative computation.

Material	ε'	ε''
X	2.0	2.2
Y	6.0	2.8
Z	10.0	0.01

TABLE 3. Volume fractions of two polymers (V_1 for $C_{22}E_1$ and V_2 for $C_{18}E_{120}$) and one conventional material (V_3 for X or Y or Z) that are necessary for production of composites with complex permittivity ε_m.

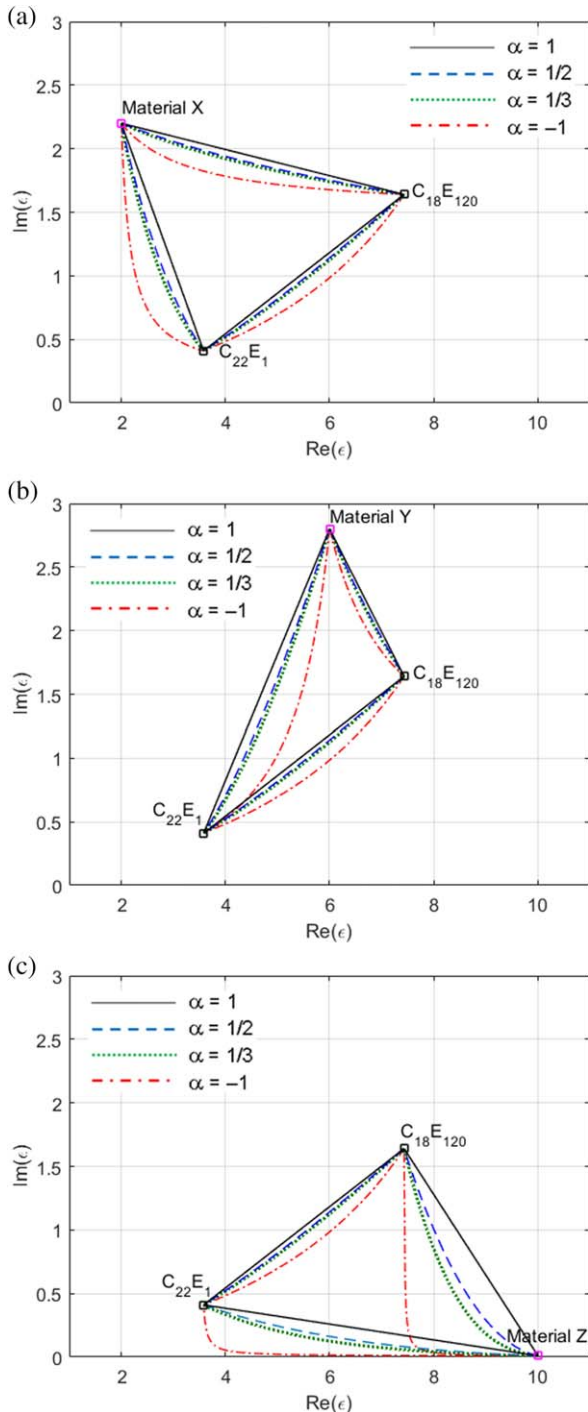| Target mixture	Domain in Fig. 2a: $\varepsilon_m = 4 - j1.5$			Domain in Fig. 2b: $\varepsilon_m = 6 - j2.0$			Domain in Fig. 2c: $\varepsilon_m = 7 - j0.5$		
α	V_1	V_2	V_3	V_1	V_2	V_3	V_1	V_2	V_3
1	0.417	0.280	0.303	0.505	0.311	0.184	0.409	0.206	0.385
1/2	0.415	0.367	0.218	0.572	0.286	0.142	0.338	0.389	0.273
1/3	0.409	0.398	0.193	0.595	0.276	0.129	0.295	0.473	0.233
−1	0.294	0.650	0.056	0.783	0.169	0.048	0.013	0.927	0.060

FIG. 2. Allowable domains for the target complex permittivity $\varepsilon_m' - j\varepsilon_m''$ for polymers $C_{22}E_1$ and $C_{18}E_{120}$ and Materials X (a), Y (b), and Z (c) for different α in model (2). [Color figure can be viewed at wileyonlinelibrary.com]

complex permittivity), for example, with a substance X, or Y, or Z in Table 2.

The allowable domains formed by these prime materials are determined by formulas (4) as curvilinear triangles shown in Fig. 2. If the required value of complex permittivity is within such a domain, then model (2) results in physically meaningful values of volume fractions of the prime materials. Examples of computed sets V_i, $i = 1, 2, 3$, are given in Table 3 for three target points ε_m in different allowable domains and for α corresponding to four different models (1).

Once the volume fractions are computed and the value of α is chosen, corresponding composite can be manufactured with the use of a production technique appropriate for the prime materials involved; complex permittivity of the resultant sample is then verified by measurement.

The capability to measure ε' and ε'' can also "calibrate" model (2) by finding the value of α most adequately representing the production process. In theory, α is conditioned by the physics behind the model (e.g., by the type of substances used in the mixture, the topology of the resulting material, etc.) [21,23,24], so in practice, with the given prime materials, α is the matter of choice. When for a series of two- and/or three-component mixtures with known volume fractions the values of ε' and ε'' are found both from (1) and measurement, α can be found as the best fit.

EXPERIMENTAL

In the experimental demonstration, we use mixtures based on three prime materials: a polymer matrix (PMMA) and two inorganic powders, silicon and aluminum oxide. Using the fillers with largely higher ε' and ε'', we intend to make an extended allowable domain and test the capability of the technique of reaching in the resulting material the values of complex permittivity notably exceeding the ones of typical polymers.

Constitutive Prime Materials

PMMA (a.k.a. as acrylic glass or plexiglass) (Struers ClaroFast), Silicon (Si, Sb-doped, particles 36–120 μm, Freiberger NE-Metall GmbH, Freiberg, Germany) and Aluminum oxide (a.k.a. as alumina) (Al_2O_3, (99.5%, particles 5–25 μm, powder 4005.0, Praxair Abler,) were used in this work.

Preparation of PMMA-Based Composites

PMMA powder was dried at 35°C for 2 h and stored in a dry atmosphere. The powders were weighted to achieve the required volume fractions and mechanically stirred until a homogeneous
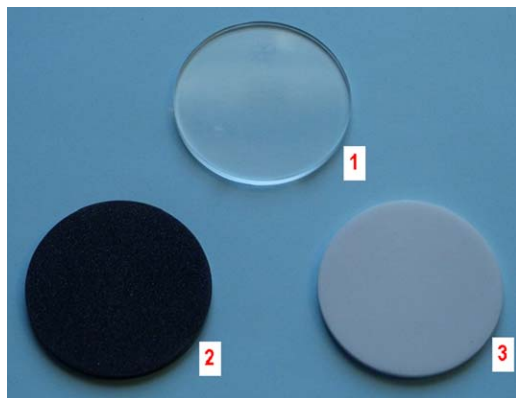
FIG. 3. Solid cylindrical disks made by hot-pressing of pure PMMA powder (1) and binary mixture powders: PMMA + Si (2), and PMMA + Al$_2$O$_3$ (3). [Color figure can be viewed at wileyonlinelibrary.com]

TABLE 4. Dielectric constant and the loss factor of the prime materials.

Materials	ε'	ε''
PMMA	2.543	0.026
Si	148.6	88.38
Al$_2$O$_3$	12.50	0.339

mixture was obtained. The mixture was heated to 180°C and compacted using uniaxial hot pressing (Hydropress-A, Jean Wirtz) for 14 min while maintaining a pressure of 45 Bars. The produced disks had diameter 50 mm and thickness of either 1 ± 0.05, or 3 ± 0.05 mm. After cooling a fine mechanical polishing was applied on both faces.

Homogeneity of the obtained samples (and thus homogeneity of the initial powder mixtures) was evaluated/controlled visually by making sure that the PMMA-based disks were uniformly transparent, the binary PMMA + Si and PMMA + Al$_2$O$_3$ composites were uniformly black and white, respectively, and the composites made of all three powders were uniformly greyish-black.

Uniformity in mixing prime powders is important and should be ensured at this step as concentrations of particles of different sizes in different areas and type of percolation may lead to dielectric properties diverged from what the power-law mixing rule predicts. A high level of homogeneity of the prepared mixtures was indirectly confirmed by low deviations of ε' and ε'' in measurements of one sample that are mentioned in the next sub-section.

Composites Characterization

Dielectric properties (i.e., dielectric constant ε' and the loss tangent $\tan\delta = \varepsilon''/\varepsilon'$) of the compacts were evaluated at room temperature using a split-post resonator method [34,35] at 2.493 GHz. Each produced sample was measured two or three times; the values of ε' and ε'' of the sample were determined as average values. Average deviations of measured values were found to be 1.2% and 2.4% for ε' and ε'', respectively.

In measurement of ε' by that technique, the main source of error is associated with uncertainty of thickness of the sample. For the produced composite disks, the maximum error is therefore estimated to be not more than $E_1 = 5.2\%$. Uncertainty in measurement of $\tan\delta$ depends on many factors, including accuracy in measurement of the Q-factor. For a properly chosen thickness of the sample and accuracy of the Q-factor measurements of $E_2 \sim 1\%$, the uncertainty in determination of the loss tangent is estimated to be 2×10^{-5}.

RESULTS AND DISCUSSION

Determination of Complex Permittivity of the Prime Materials

Computation of volume fractions by model (2) requires that dielectric constant and the loss factor of the prime materials are to

be known. In this article, in the absence of a reliable measurement technique applicable to the PMMA, silicon, and alumina powders (characterized by considerably different values of ε' and ε''), their dielectric properties were found by measuring corresponding hot-pressed cylindrical disks. We determined dielectric properties of

I. PMMA powder by measuring the polymer compact made from PMMA powder, and
II. Si and Al$_2$O$_3$ powders by (a) measuring the composite compacts made from binary mixtures of Si and Al$_2$O$_3$ with PMMA, and (b) calculating ε' and ε'' of Si and Al$_2$O$_3$ powders from (1) with $n = 2$.

Two pure PMMA compacts and seven binary mixture compacts were produced – including four by adding Si (in volume fractions from 0.0148 to 0.1375) and three by adding Al$_2$O$_3$ (in volume fractions from 0.0595 to 0.1434) to the PMMA environment; these compacts are exemplified in Fig. 3.

The values of ε' and ε'' of silicon and alumina powders were calculated for values of α in the range from 0.3 to 0.6 and then used in (1) (also for $0.3 \leq \alpha \leq 0.6$) for computing complex permittivity of four composite compacts produced by adding both silicon powder (in volume fractions from 0.0574 to 0.1312) and alumina powder (in volume fractions from 0.0575 to 0.1388) to the PMMA environment. Dielectric properties of these four composites were also measured. It turned out that the values of ε' computed with $\alpha = 0.373$ and ε'' computed with $\alpha = 0.365$ were the closest to the measured ones. This illustration of "calibration" of the computational part of the proposed technique gives us a motivation to adopt the inverted Looyenga model [i.e., $\alpha = 1/3$ in (2)] for determining the volume fraction of the PMMA, Al$_2$O$_3$, and Si composites.

Analyzing the resulting values of complex permittivity for all three prime materials (Table 4), one can notice that for PMMA, the values of dielectric constant and the loss factor are very close to the data for plexiglass ($\varepsilon' = 2.59$–2.75 and $\varepsilon'' = 0.0009$–0.0015) at 2.4 GHz reported in [36,37], and our results for alumina seem to be consistent with the data [38] estimating ε' and ε'' of sapphire in the range of 1–10 GHz to be of order 9–10 and 10^{-4}, respectively. Data on complex permittivity of silicon powder is not commonly available, but dielectric constant and the loss factor of silicon wafers are known to be very different for *n*- and *p*-types of silicon and strongly dependent on doping; for instance, the data in [39–42] indicates that the loss factor can be expected to take on any value in the interval from 50 to 500, and that is consistent with our result (88.4). We therefore conclude that the values of ε' and ε'' in Table 4 are sufficiently plausible for the purpose of demonstration of functionality of the technique presented in this article.

Composite with Required Complex Permittivity

Here we describe the experiment in production of the PMMA-Si-Al$_2$O$_3$ composites as the materials with required

TABLE 5. PMMA-Si-Al$_2$O$_3$ composites—computational and experimental results.

| Sample (Fig. 4) | Required complex permittivity | | Volume fractions of PMMA (V_1), Si (V_2), and Al$_2$O$_3$ (V_3) | | Complex permittivity of the produced sample: | | | |
| | | | | | Model (1), $\alpha = 1/3$ | | Measurement | |
	ε'	ε''	Model (2), $\alpha = 1/3$	Used in production	ε'	ε''	ε'	ε''
A	6.0	0.2	0.6496	0.6696	5.74	0.183	5.88	0.198
			0.0394	0.0369				
			0.3110	0.2935				
B	4.0	0.1	0.8598	0.8587	4.01	0.101	3.89	0.057
			0.0297	0.0298				
			0.1104	0.1115				
C	6.0	0.3	0.7547	0.7564	5.96	0.294	5.88	0.211
			0.0731	0.0722				
			0.1722	0.1714				
D	6.5	0.3	0.6777	0.6839	6.39	0.289	5.85	0.167
			0.0649	0.0633				
			0.2574	0.2528				
E	7.0	0.4	0.6882	0.6937	6.88	0.385	6.44	0.227
			0.0840	0.0820				
			0.2279	0.2243				

complex permittivity. First, the inverted Looyenga model (2) was used with the data on ε' and ε'' of the prime materials (Table 4) to determine the volume fractions in which the three powders should be taken to produce five samples A to E (introduced in the first three columns of Table 5). The values of their complex permittivity were chosen to be in the allowable domain for the used prime materials (Fig. 4). The computed values of V_1, V_2, V_3 are collected in Table 5 along with corresponding values of the volume fractions in which the powders were actually taken in production of those samples (4th and 5th columns). Those experimental values were then tested with the direct Looyenga model (1) to evaluate the occurred change in complex permittivity; the computed values of ε' and ε'' are collected in the 6th and 7th columns. Then five composites were hot-pressed as thin disks; the resulting samples are shown in Fig. 5, and their measured dielectric constant and the loss factor are given in the right two columns of Table 5.

FIG. 4. A section of the allowable domain for PMMA, Al$_2$O$_3$ and Si powders as the prime materials with points representing targeted (*) and produced (o) complex permittivity. [Color figure can be viewed at wileyonlinelibrary.com]

Analysis of the Results

Comparing the values of the targeted and produced complex permittivity in Table 5, one can see that while there is an excellent agreement in dielectric constants (the divergence does not exceed 4.3%), the values of the loss factor are close enough in one Case (8%, Sample A), but notably diverge in the others (about 40%, Samples B, D, E). This disagreement may be explained by a number of factors related to the implementation of the proposed technique, and the following four appear to be most influential.

- Complex permittivity of the silicon and alumina powders (Table 4) were determined not by a direct measurement, but by measurement of the binary solid composites produced by mixing these powders into the PMMA environment and hot-pressing it, and subsequent computation of dielectric constant and the loss factor by the inverted model (2).
- While the role of silicon powder is crucial in examination of capability of the technique in reaching in the resulting composites high values of ε'_m, complex permittivity of that substance, being very high, is quite sensitive to many physical parameters including density; one therefore may suggest that
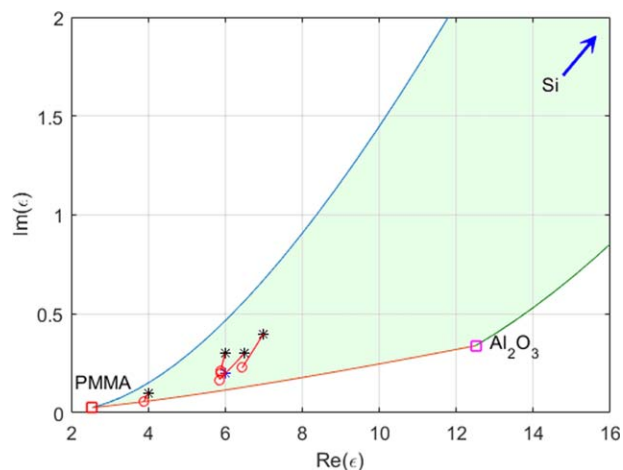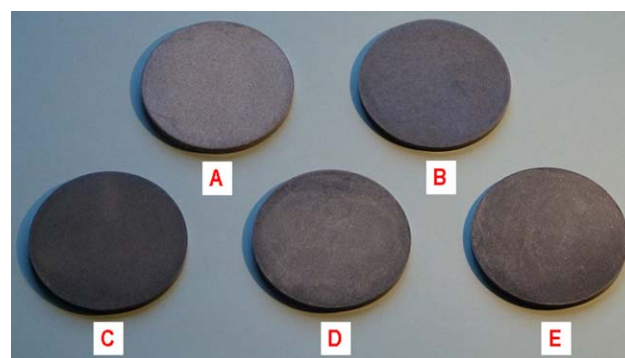

FIG. 5. Samples of PMMA-Si-Al$_2$O$_3$ composites (Table 5) produced as the materials with required complex permittivity. [Color figure can be viewed at wileyonlinelibrary.com]

TABLE 6. Average uncertainties in computation of complex permittivity of silicon and alumina powders with model (1) ($\alpha = 1/3$) due to error propagation.

	Silicon powder		Alumina powder	
	ε'	ε''	ε'	ε''
Table 4	148.49	87.64	12.50	0.331
δ	± 70.18	± 11.12	± 6.14	± 0.134
δ (%)	51.7	20.0	47.4	37.7

the values of ε' and ε'' computed from the measured complex permittivity of the PMMA-Si compacts may insufficiently adequately represent ε' and ε'' of this prime powder material.

- The power-law mixing rule (1) [and therefore its inverted version (2)] is known to be less accurate for low values of V_2 and V_3 [23]; in our experiment, as recorded in Table 5, volume fractions of silicon powder (whose ε'' is more than three orders of magnitude higher than the one of PMMA) is particularly low (0.03–0.08).
- Determination of volume fractions of the prime substances requires computation with both models (1), (2) which use the experimental data of ε' and $\tan\delta$ measured with inevitable uncertainty. This requires taking into account the effect of error propagation. Uncertainties δ in computing complex permittivity of silicon and alumina powders from measurement of the binary composite compacts (model (2), $n = 2$) were determined by formulas (A2) and are collected in Table 6. Uncertainties in computing complex permittivity of the PMMA-Si-Al$_2$O$_3$-composites by model (1) with $n = 3$ were determined by formulas (A4). The average (for four composite samples) uncertainties in computing ε' and ε'' turned out to be 14.6% and 8.4%, respectively. As model (2) with $n = 3$ requires Gaussian elimination [and apparently more arithmetic operations than the direct model (1)], it is clear that error propagation can make a notable impact on computation of V_i as well.

Considering all these factors potentially affecting the performance, one can conclude that the observed deviations of the resulting ε''_m fall into the anticipated ranges, and the presented results confirm the validity and functionality of the suggested approach to production of materials with required complex permittivity.

Regarding the examining the technique in reaching in the resulting composite higher values of dielectric constant and the loss factor, in accordance with the computational part of the technique, this goal is achievable as long as the target value is located in the allowable domain on the complex permittivity plane. In the implementation reported in this article, however, that option is limited by the capability of the production method: our technique of hot-pressing (associated with preceding mechanical mixing) makes ceramic-polymer composites and remains operational for relatively low presence of ceramic fillers in the polymer environment (in our experiments, not more than 35%). As such, with the volume fraction of silicon powder not exceeding 0.084, the highest value of complex permittivity for the resulting composite, compared to the PMMA compact (2.54 – j0.026), was 7.0 – j0.4.

CONCLUSIONS

A computational procedure and a process of production of materials with required complex permittivity have been described and demonstrated for a group of ceramic-polymer composites. The technique is based on inversion of the power-law mixing rule for three materials; it determines the volume fractions of those substances which, after thoroughly mixing, are expected to end up in the material with the targeted dielectric constant and the loss factor. Functionality of the technique, after "calibration" of model (2), has been presented for the Looyenga (a.k.a. Landau-Lifshitz) model (with the power $\alpha = 1/3$) applied to silicon and alumina powders mixed into the PMMA environment and hot-pressed into a set of polymer composites. The resulting dielectric constants of the produced composites are in excellent agreement with the ones suggested by the model.

The key factors contributing to a notable divergence of the loss factor are conditioned by the features of the presented implementation of the technique. Silicon powder (chosen to enforce capabilities of the technique in reaching higher values of ε'_m) has an utmost uncertainty in its complex permittivity (especially, in the loss factor) and also worsens the accuracy of model prediction by being present in the mixture in very small portions. So, for a prime powder which, as silicon powder, is characterized by high value of complex permittivity, experimental verification of the produced ε' and ε'' is needed to confirm that their values are not quite far from the desired ones. Anyway, regarding ε''_m, performance of our technique is expected to significantly improve when using prime materials with similar molecular structures (e.g., all polymers) characterized by not very different (and known from reliable measurement) values of complex permittivity.

If the approach described in this article is used to make the material required by the optimization technique [13,14], the divergence of the produced ε' and ε'' from the optimal ones could be compensated by additional optimization of geometrical parameters for the fixed (actually produced) complex permittivity. Moreover, the presented demonstration of functionality of the proposed technique with polymer composites may suggest formulations of optimization problems seeking for the optimal materials with low values of ε''.

For larger pieces of polymer composites with required complex permittivity, the technique will need a larger press, but the computational procedure and conditions for its operation will require no change. For the resulting material with much higher values of dielectric constant, appropriate production technique for production of ceramic composites will be needed (for examples, from the components with similar molecular structures, like Li-Nb-Ti-O ceramics [43]), but, again, the concept and basic principles of the underlying modeling may hold.

On the computational side of the technique, further development may be needed to handle the case of four or more prime materials. In this case, model (2) becomes an underdetermined system, and there may be the need to solve an optimization problem subject to linear equality constraints to find physically meaningful solutions. Conversely, while the Looyenga model (also called the "permittivity of a mixture" [30]), being symmetrical with respect to the inclusion and environment, seems to be most accurate and physically most suitable for mixtures of powders, other models (though involving a reasonable number of arithmetic operations not to amplify the effect of error propagation) appropriate for other prime types of materials and other topologies of the mixtures (such as the Maxwell-Garnett model and the Bruggeman nonsymmetric formula [21]) may be explored.

APPENDIX

With $n = 2$, model (1) represents the power-rule mixing model for two materials. Since complex permittivity of only PMMA (Material 1) is measured, complex permittivity of Si (Material 2) and Al_2O_3 (Material 3) can be calculated by re-writing (1) for $\varepsilon_{2,3}$. In this form, it becomes a function of four measured characteristics: ε' and $\tan\delta$ of Materials 1 and the mixtures of Material 1 with Material 2/3. For the adopted Looyenga model, $\alpha = 1/3$ and the inverted model (1) appears in the form:

$$\varepsilon'_{2,3} = f_1(\varepsilon'_1, \varepsilon'_m) = \left(\frac{1}{V_{2,3}}\varepsilon'^{\frac{1}{3}}_m - \frac{V_1}{V_{2,3}}\varepsilon'^{\frac{1}{3}}_1\right)^3, \qquad (A1a)$$

$$\varepsilon''_{2,3} = f_2(\varepsilon'_1, T_1, \varepsilon'_m, T_m) = \left(\frac{1}{V_{2,3}}(\varepsilon'_m T_m)^{\frac{1}{3}} - \frac{V_1}{V_{2,3}}(\varepsilon_1 T_1)^{\frac{1}{3}}\right)^3 \qquad (A1b)$$

where $T_1 = (\tan\ \delta)_1$ and $T_m = (\tan\ \delta)_m$. Following [44], uncertainties in computing the real and imaginary parts of complex permittivity of Material 2/3 can be found from the following expressions:

$$\delta\varepsilon'_{2,3} = \sqrt{\left(\frac{\partial\varepsilon'_{2,3}}{\partial\varepsilon'_1}\delta\varepsilon'_1\right)^2 + \left(\frac{\partial\varepsilon'_{2,3}}{\partial\varepsilon'_m}\delta\varepsilon'_m\right)^2}, \quad \delta\varepsilon''_{2,3} = \sqrt{\left(\frac{\partial\varepsilon''_{2,3}}{\partial\varepsilon'_1}\delta\varepsilon'_1\right)^2 + \left(\frac{\partial\varepsilon''_{2,3}}{\partial T_1}\delta T_1\right)^2 + \left(\frac{\partial\varepsilon''_{2,3}}{\partial\varepsilon'_m}\delta\varepsilon'_m\right)^2 + \left(\frac{\partial\varepsilon''_{2,3}}{\partial T_m}\delta T_m\right)^2}.$$

After finding the derivatives of functions (A1), the last two formulas for uncertainties of determination of dielectric constant and the loss factor of Material 2/3 are reduced to the forms:

$$\delta\varepsilon'_{2,3} = \frac{1}{V_{2,3}}\left(\frac{1}{V_{2,3}}\varepsilon'^{\frac{1}{3}}_m - \frac{V_1}{V_{2,3}}\varepsilon'^{\frac{1}{3}}_1\right)^2\sqrt{\frac{V_1^2}{\varepsilon'^{\frac{4}{3}}_1}(\delta\varepsilon'_1)^2 + \frac{1}{\varepsilon'^{\frac{4}{3}}_m}(\delta\varepsilon'_m)^2}$$

$$\hspace{10cm}(A2a)$$

$$\delta\varepsilon''_{2,3} = \frac{1}{V_{2,3}}\left(\frac{1}{V_{2,3}}(\varepsilon'_m T_m)^{\frac{1}{3}} - \frac{V_1}{V_{2,3}}(\varepsilon'_1 T_1)^{\frac{1}{3}}\right)^2$$

$$\times\sqrt{\frac{V_1^2 T_1^{\frac{2}{3}}}{\varepsilon'^{\frac{4}{3}}_1}(\delta\varepsilon'_1)^2 + \frac{V_1^2\varepsilon'^{\frac{2}{3}}_1}{T_1^{\frac{4}{3}}}(\delta T_1)^2 + \frac{T_m^{\frac{2}{3}}}{\varepsilon'^{\frac{4}{3}}_m}(\delta\varepsilon'_m)^2 + \frac{\varepsilon'^{\frac{2}{3}}_m}{T_m^{\frac{4}{3}}}(\delta T_m)^2}$$

$$\hspace{10cm}(A2b)$$

Input data for formulas (A2) are the values of ε'_1, ε'_m, $(\tan\ \delta)_1$, V_1, V_2, and V_3 taken from the experiment and the uncertainties $\delta\varepsilon'_1$, $\delta\varepsilon'_m$ and $\delta(\tan\ \delta)_1$ calculated, following section *Composites Characterization* above, for $E_1 = 5.2\%$ and $E_2 = 1.0\%$.

With $n = 3$, model (1) represents the power-rule mixing model for three materials. Complex permittivity of PMMA (Material 1) is known from measurement, and complex permittivity of Si and Al_2O_3 (Materials 2 and 3) are determined from the inverted model (A1a,b). In this case, model (1) (with $\alpha = 1/3$) appear in the form:

$$\varepsilon'_m = F_1(\varepsilon'_1, \varepsilon'_2, \varepsilon'_3) = \left(V_1\varepsilon'^{\frac{1}{3}}_1 + V_2\varepsilon'^{\frac{1}{3}}_2 + V_3\varepsilon'^{\frac{1}{3}}_3\right)^3 \qquad (A3a)$$

$$\varepsilon''_m = F_2(\varepsilon'_1, T_1, \varepsilon''_2, \varepsilon''_3) = \left(V_1(\varepsilon'_1 T_1)^{\frac{1}{3}} + V_2\varepsilon''^{\frac{1}{3}}_2 + V_3\varepsilon''^{\frac{1}{3}}_3\right)^3 \qquad (A3b)$$

Similarly to the derivation of (A2), the formulas for the uncertainties of determination of dielectric constant and the loss factor of the mixture appear as follows:

$$\delta\varepsilon'_m = \left(V_1\varepsilon'^{\frac{1}{3}}_1 + V_2\varepsilon'^{\frac{1}{3}}_2 + V_3\varepsilon'^{\frac{1}{3}}_3\right)^2$$

$$\times\sqrt{\frac{V_1^2}{\varepsilon'^{\frac{4}{3}}_1}(\delta\varepsilon'_1)^2 + \frac{V_2^2}{\varepsilon'^{\frac{4}{3}}_2}(\delta\varepsilon'_2)^2 + \frac{V_3^2}{\varepsilon'^{\frac{4}{3}}_3}(\delta\varepsilon'_3)^2}$$

$$\hspace{8cm}(A4a)$$

$$\delta\varepsilon''_m = \left(V_1\varepsilon'^{\frac{1}{3}}_1 T_1^{\frac{1}{3}} + V_2\varepsilon''^{\frac{1}{3}}_2 + V_3\varepsilon''^{\frac{1}{3}}_3\right)^2$$

$$\times\sqrt{\frac{V_1^2\varepsilon'^{\frac{2}{3}}_1}{T_1^{\frac{4}{3}}}(\delta T_1)^2 + \frac{V_1^2 T_1^{\frac{2}{3}}}{\varepsilon'^{\frac{4}{3}}_1}(\delta\varepsilon')^2 + \frac{V_2^2}{\varepsilon''^{\frac{4}{3}}_2}(\delta\varepsilon''_2)^2 + \frac{V_3^2}{\varepsilon''^{\frac{4}{3}}_3}(\delta\varepsilon''_3)^2}$$

$$\hspace{8cm}(A4b)$$

Input data for formulas (A4) are the values of ε'_1, $(\tan\ \delta)_1$, V_1, V_2, and V_3 taken from the experiment, ε'_2, ε''_2, ε'_3, ε''_3—from computation with model (1) ($n = 3$), and the uncertainties $\delta\varepsilon'_1$, and $\delta(\tan\ \delta)_1$ – from calculations summarized in Table 6; all the uncertainties here are also determined for $E_1 = 5.2\%$ and $E_2 = 1.0\%$.

REFERENCES

1. H.S. Nalwa, *Handbook of Low and High Dielectric Constant Materials and Their Applications*, Academic Press, London, UK (1999).

2. K. Fenske and D. Misra, *Appl. Microwave Wireless*, **12**, 92 (2000).

3. J.C.J. Bart, *Additives in Polymers: Industrial Analysis and Applications*, Wiley, New York (2005).

4. P. Puligundla, S.A. Abdullah, W. Choi, S. Jun, S.-E. Oh, and S. Ko, *J. Food Process. Technol.*, **4**, 1000278 (2013).

5. H.J. Kitchen, S.R. Vallance, J.L. Kennedy, N. Tapia-Ruiz, L. Carassiti, A. Harrison, A.G. Whittaker, T.D. Drysdale, S.W. Kingman, and D.H. Gregory, *Chem. Rev.*, **114**, 1170 (2014).

6. T. Yoshimura, T. Suzuki, S. Mineki, and S. Ohuchi, *PLoS One*, **10**, e0136532 (2015).

7. V.V. Yakovlev, *AMPERE Newslett.*, **89**, 18 (2016).

8. C. Fernández-Martín, *AMPERE Newsletter*, **90**, 19 (2016).

9. N.M. Gerbo, D. Boldor, and C.M. Sabliov, *J. Microwave Power Electromag. Energy*, **42**, 55 (2007).

10. K.P. Nott, L.D. Hall, J.R. Bows, M. Hale, and M.L. Patrick, *Intern. J. Food Sci. Technol.*, **34**, 305 (1999).

11. K. Knoerzer, M. Regier, E.H. Hardy, H.P. Schuchmann, and H. Schubert, *Innovative Food Sci. Emerg. Technol.*, **10**, 537 (2009).

12. D. Zymelka, S. Saunier, J. Molimard, and D. Goeuriot, 12th Seminar Computer Modeling in Microwave Engineering & Applications – Advances in Modeling of Microwave Sintering, Grenoble, France, March 38 (2010).

13. J.T. Bernhard and W.T. Joines, *IEEE Trans. Microwave Theory Tech.*, **44**, 457 (1996).

14. K.A. Lurie and V.V. Yakovlev, *J. Eng. Math.*, **44**, 107 (2002).

15. E.M. Moon, J.F. Gerling, C.W. Scouten, and V.V. Yakovlev, Proc. 49th IMPI's Microwave Power Symp., San Diego, CA, 54 (2015).

16. E.M. Moon, and V.V. Yakovlev, Proc. 3rd Global Congress on Microwave Energy Applications, Cartagena, Spain, 224 (2016).

17. K. Werner, *Microwave J.*, **58**, 22 (2015).

18. X. Hao, *J. Adv. Dielect.*, **03**, 1330001 (2013).

19. G.G. Raju, *Dielectrics in Electric Fields*, 2nd ed., CRC Press, Boca Raton, FL, 2017.

20. B. Galindo, A. Benedito, F. Ramos, and E. Gimenez, *Polym. Eng. Sci.*, **56**, 1321 (2016).

21. A. Sihvola, *Electromagnetic Mixing Formulas and Applications*, IFT, London, UK (1999).

22. M. Wang and N. Pan, *Mater. Sci. Eng. R*, **63**, 1 (2008).

23. J. Sheen, Z.-W. Hong, C.-W. Su, and H.-C. Chen, *Prog. Electromagn. Res.*, **100**, 13 (2010).

24. E.M. Kiley, V.V. Yakovlev, K. Ishizaki, and S. Vaucher, *J. Microwave Power Electromagn. Energy*, **46**, 26 (2012).

25. A.V. Goncharenko, V.Z. Lozovski, and E.F. Venger, *Opt. Commun.*, **174**, 19 (2000).

26. K. Lichtenecker, *K. Phys. Zeitschrift.*, **27**, 115 (1926).

27. J.R. Birchak, L.G. Gardner, J.W. Hipp, and J.M. Victor, *Proc. IEEE*, **62**, 93 (1974).

28. A. Kraszewski, *J. Microwave Power*, **12**, 215 (1977).

29. H. Looyenga, *Physica*, **31**, 401 (1965).

30. L.D. Landau and E.M. Lifshitz, *Electrodynamics of Continuous Media*, Pergamon Press, Oxford, UK (1960).

31. K. Wakino, *Proc. IEEE Int. Symp. on Applications of Ferroelectrics*, 33 (1994).

32. S.A. Stolzle, A. Enders, and G. Nimtz, *J. Phys. I*, **2**, 401 (1999).

33. Y. Yamada Pittini, D. Daneshvari, R. Pittini, S. Vaucher, L. Rohr, S. Leparoux, and H. Leuenberger, *Eur. Polym. J.*, **44**, 1191 (2008).

34. J. Krupka, R.N. Clarke, O.C. Rochard, and A.P. Gregory, 13th Int. Conf. Microwaves, Radar and Wireless Communications (MIKON-2000), Wrocław, Poland, (2000)10.1109/MIKON.2000.913930.

35. J. Krupka, A.P. Gregory, O.C. Rochard, R.N. Clarke, B. Riddle, and J. Baker-Jarvis, *J. Eur. Ceram. Soc.*, **21**, 2673 (2001).

36. J. Musil and F. Žácek, *Microwave Measurements of Complex Permittivity by Free Space Methods and Their Applications*, Elsevier, New York (1986).

37. R. Wilson, *Propagation Losses Through Common Building Materials – 2.4 GHz vs 5 GHz*, Magis Networks, Inc., San Diego, CA (2002).

38. A. Nakayama, A. Fukuura, and M. Nishimura, *IEEE Trans. Microwave Theory Tech.*, **51**, 170 (2003).

39. J.D. Holm and K.S. Champlin, *J. Appl. Phys.*, **39**, 275 (1968).

40. P.K. Roy and A.N. Datta, *IEEE Trans. Microwave Theory Tech.*, **37**, 144 (1974).

41. N.H. Baba, Z. Awang, and D.K. Ghodgaonkar, 2003 Asia-Pacific Conf. Applied Electromagnetics (APACE 2003), Shah Alam, Malaysia, 119.

42. S.K. Varadan, "*Estimation of Complex Permittivity of Silicon at 2.45 GHz Microwave Frequency*," M.S. Thesis, Arizona State University (2014).

43. Z. Liu, Y. Wang, W. Wu, and Y. Li, *J. Asian Ceram. Soc.*, **1**, 2 (2013).

44. J.R. Taylor, *An Introduction to Error Analysis*, 2nd ed., University Science Books, Herndon, VA (1997) .